Ultrasonically Induced Au Nanoprisms and Their Size Manipulation Based on Aging

Cuncheng Li, Weiping Cai,* Yue Li, Jinlian Hu, and Peisheng Liu

Key Laboratory of Material Physics, Anhui Key Laboratory of Nanomaterials and Nanotechnology, Institute of Solid State Physics, Chinese Academia of Sciences, Hefei, 230031, Anhui, P. R. China

Received: September 28, 2005; In Final Form: November 24, 2005

A simple sonochemical approach was developed for the synthesis of single-crystal Au nanoprisms with triangular or hexagonal shape, 30−40 nm planar dimension, and 6−10 nm thickness in an ethylene glycol solution. It has been shown that ethylene glycol, the surfactant poly(vinylpyrrolidone), and ultrasonic irradiation play important roles in the formation of Au nanoprisms. The subsequent aging induces the growth of Au nanoprisms, which is attributed to the existence of residual reduced Au° atoms and Au clusters in the solution. Further growth of Au nanoprisms could be realized by adding a given amount of $HAuCl_4$ to the irradiated and aged Au nanodisk colloidal solution, which provides a simple and an effective method to synthesize Au nanoprisms with different sizes. Au nanoprisms with planar sizes from 70 to 400 nm have been successfully synthesized based on this strategy.

1. Introduction

Fabrication of metal nanostructures has been an active research area for several decades, because of their unique properties different from their bulk counterparts and important applications in catalysis, optics, electronics, and biodiagnostics.[1] Much effort has been devoted to synthesize spherical and rodlike metal nanostructures. Recently, synthesis of platelike metal nanostructures, such as, nanosheets,[2] nanoprisms,[3,4] nanodisks,[5−9] and nanorings,[10] has also received considerable attention, mainly due to their unusual optical properties and potential applications. For example, the field-enhancement effect, near the triangle tips of a metal nanoprism, makes it have important applications in atomic force microscopy (AFM), scanning tunneling microscope (STM), and scanning near-field optical microscopy (SNOM).[3,11] Au nanoprisms, with extremely flat surface and large near-infrared (NIR) absorption, are regarded as a very effective and a convenient substitute for Au−SiO_2 core−shell nanostructures in cancer hyperthermia.[3] This has thus led to an explosion of interest in the development of synthetic approaches to prepare such metal nanostructures. Until now, several synthesis strategies, including photochemistry,[5a,5b,12] thermochemistry,[2,5c,8b,9,13] wet-chemistry,[4,7,8a,14] and biochemistry,[3,15] have been developed. Among these, size control of metal nanoprisms, which is important to uncover their size-dependent properties and to achieve their practical applications, is usually realized via the experimental parameters.

Here, we report a simple sonochemical approach to synthesize single-crystal Au nanoprisms with planar dimension 30−40 nm in an ethylene glycol solution. Their sizes can be manipulated in the range of 70−400 nm via the subsequent processes at room temperature.

2. Experimental Section

In a typical synthesis of Au nanoprisms, 1.11 g of poly(vinylpyrrolidone) (PVP, K-30, $M_w = 40\,000$, Aldrich) was first added to 50 mL of ethylene glycol (Aldrich) solution in a conical flask. The mixed solution was stirred under a magnetic blender for about 15−20 min, followed by dropping 0.1 mL of $HAuCl_4$ aqueous solution (Aldrich, 250 mM). The concentrations of $AuCl_4^-$ ions and PVP in the mixed solution were 0.5 and 200 mM, respectively. The yellow color appeared in the solution due to the $AuCl_4^-$ ions. Subsequently, the flask was mounted at a constant position in a sonication bath and ultrasonically irradiated for a certain time, on a JL 360 commercial ultrasonic cleaner operating at the frequency 45 ± 2.5 kHz and with a power 2.4 W/cm^2, respectively. During ultrasonic irradiation, the flask was purged with argon gas to eliminate the oxygen in it, as illustrated in Figure 1. The temperature in the sonication bath was kept at about 25 °C by circulated water.

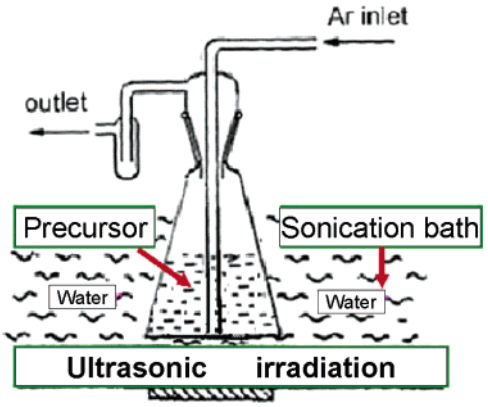

Figure 1. Schematic illustration of an ultrasonically irradiated process.

The optical absorption spectra were measured for all samples on a Cary 5E UV−vis−NIR spectrophotometer in the wavelength range from 250 to 1250 nm, using an optical quartz cell with a 10 mm path length. The samples for transmission electron microscopic (TEM) examination were prepared by putting a droplet of the treated solution on the copper grids coated with thin carbon film and evaporating it in air at room temperature. TEM observation was conducted on a JEOL 2010 TEM, operating at an accelerating voltage of 200 kV.

* To whom correspondence should be addressed. E-mail: wpcai@issp.ac.cn.

10.1021/jp055522l CCC: $33.50
Published on Web 01/06/2006

3. Results

3.1. Ultrasonically Induced Au Nanoprisms. Figure 2 A shows the optical absorption spectra of the $HAuCl_4$ ethylene glycol solution after ultrasonic irradiation for a different time. Before irradiation, there is one absorption peak at 322 nm, which is a unique "fingerprint" for $AuCl_4^-$ ions and directly originates from the d−d transition of the $AuCl_4^-$ ions.[16] The absorption peaks around 920, 1000, and 1200 nm are from pure ethylene glycol and not discussed here (see curve a in Figure 2A). The absorption peak ever decreases and disappears after 90 min, indicating a complete reduction of $AuCl_4^-$ ions. A broad, weak absorption band at 550 nm, a well-known surface plasmon resonance (SPR) peak of Au nanoparticles,[17] appears when ultrasonic irradiation occurs for 50 min, which indicates that Au nanoparticles have been produced. This absorption band gradually enhances with a rise in ultrasonic-irradiation time. At 70 min, another absorption peak at 670 nm can be observed. Further irradiation leads to an increase in both peaks, together with shifting to 545 and 690 nm, respectively, showing the formation of either anisotropic or aggregated Au nanoparticles.[3,8]

The corresponding TEM observation demonstrates the formation of Au nanoprisms. Parts B−D of Figure 2 illustrate Au nanostructures at three typical stages of the ultrasonic process (50, 70, and 120 min, respectively). After irradiated for 50 min, ultrafine Au nanoparticles smaller than 5 nm were formed (see Figure 2B). After ultrasonic irradiation for 70 min, these ultrafine Au nanoparticles developed into nanoplatelets and nanoparticles 10−20 nm in size (see Figure 2C) and finally grew into Au nanoprisms together with some nanoparticles, as illustrated in parts D and E of Figure 2. The 120 min irradiated sample is mainly composed of Au nanoprisms with a triangular or hexagonal shape, 30−40 nm planar dimension, and 6−10 nm thickness. Many nanoprisms have regular edge sides with an angle of 120° (for hexagon nanodisks) or 60° (for triangle nanodisks) between adjacent sides. This is consistent with the results of the corresponding optical absorption spectra shown in Figure 2A. It is well-known that when metallic nanoparticles are not spherically shaped, but oblate, platelet, or prism, the SPR will deviate from a single-peak feature and split into two or more peaks (in- and out-of-plane plasmon resonance) due to the platelike morphology.[3−5,17] The absorption at 690 nm originates from the in-plane dipole plasmon resonance. There are two parts that contribute to the absorption at 545 nm: the normal SPR of Au nanoparticles and out-of-plane dipole resonance of Au nanoprisms, which is close to that of Au nanoparticles.[3a,8]

The selected area electron diffraction (SAED) pattern was obtained by focusing the electron beam on a single Au nanodisk lying flat on the TEM grid and is shown in Figure 2F. The inner set of spots in the [111] pattern is believed to originate from the $^1/_3${422} planes normally forbidden by a face centered cubic (fcc) lattice. According to the results of Kirkland et al.[18] and Germani et al.,[19] such $^1/_3${422} forbidden reflections observed on the platelike structures of silver or gold should be attributed to (111) stacking faults parallel to the (111) surface and extending across the entire nanoprism. Thus, it is reasonable that the top and bottom surfaces of the Au nanoprisms are bound by atomically flat {111} planes.[3,5,10] The second set of spots with the strongest intensity is indexed to {220} Bragg reflections, which indicates that the as-prepared nanoprisms are single crystal with {111} lattice planes as the basal surfaces. Also, the sidewalls of the Au nanosheets with hexagonal or triangular shape should be terminated with {110} planes concluded from the angles between the adjacent edge sides and between the {111} basal planes and the sidewalls (see parts D and E of Figure 2). Energy dispersive spectrum (EDS) analysis has confirmed that the as-prepared nanoprisms consist of only gold (see Figure 2G, carbon and copper elements come from the copper grids coated with thin carbon film).

3.2. Influence Factors. Further experiments revealed that both the ethylene glycol and the surfactant PVP with a certain concentration are important in the formation of Au nanoprisms.

If the ultrasonic solvent is the ethanol/water solution or pure aqueous solution with PVP, then only one absorption peak at 540 nm appears and increases monotonically with a rise in the ultrasonic-irradiation time. The product obtained is only composed of 10−30 nm spherical Au nanoparticles (see Figure 3). In the monoalcohol (with PVP), such as, ethanol, 2-propanol, and isopropy alcohol, instead of ethylene glycol as the ultrasonic solvent, the absorption peak of $AuCl_4^-$ ions is unchanged even after ultrasonic irradiation for more than 8 h, indicating that $AuCl_4^-$ ions cannot be reduced in these solvents via ultrasonic irradiation.

Figure 4A presents the optical absorption spectra for the samples synthesized at the same condition (ethylene glycol as the ultrasonic solvent and the concentration of $HAuCl_4$ is 0.5 mM), but with different PVP concentrations, which reveals that the concentration of PVP in the range from 100 to 200 mM induces dominant Au nanoprisms. When the PVP concentration is up to 300 mM, there is only one peak at 545 nm in the corresponding optical spectrum (curve c in Figure 3A). The product is dominated by equiaxial Au nanoparticles with irregular shape, together with very few Au nanoprisms as shown by the arrows in Figure 4B. In the absence of PVP, the reduction rate of $AuCl_4^-$ ions is very slow (needing several hours (6 h)) and the product (Au nanoparticles) is easily aggregated.

A laser-irradiation experiment (second harmonic of Nd:YAG laser; wavelength, 532 nm; energy, 80 mJ; frequency, 1 Hz; pulse width, 10 ns) was also conducted. For the $HAuCl_4$ ethylene glycol solution containing PVP (the concentrations of $HAuCl_4$ and PVP are 0.5 and 200 mM, respectively), laser irradiation induces the products of spherical Au nanoparticles 6−15 nm in size instead of Au nanoprisms, as illustrated in Figure 5. The corresponding optical absorption spectrum only shows one-mode SPR at 527 nm. This suggests that ultrasonic irradiation is also crucial to the formation of Au nanoprisms.

3.3. Size Manipulation. Time evolution of the morphology was observed at room temperature for the as-prepared Au nanoprism colloid. It is indicated that subsequent aging induces the continuous growth of Au nanoprisms. Figure 6A shows the TEM result for the 120 min ultrasonic irradiated sample after aging for one week. The size of Au nanoprisms is increased to 70−90 nm. The corresponding optical absorption spectrum shows that both the in-plane and the out-of-plane dipole absorptions of Au nanoprisms are enhanced. Moreover, the in-plane SPR peak at 690 nm red shifts to 760 nm (see Figure 6B), showing the growth of Au nanoprisms and the sensitivity of the in-plane SPR to the size. Longer aging cannot induce further growth of Au nanoprisms. Such growth is attributed to the existence of the residual reduced Au° atoms and Au clusters in the solution after ultrasonic irradiation.

Further growth of Au nanoprisms can be realized by adding a given amount of $HAuCl_4$ to the irradiated and aged colloidal solution. Figure 7A shows the time evolution of the optical spectra for the aged irradiated sample (5 mL) after an addition of 0.1 mL of 25 mM $HAuCl_4$ solution at room temperature. The absorption peak of $AuCl_4^-$ ions ever decreased and completely disappeared after one week, indicating that $AuCl_4^-$

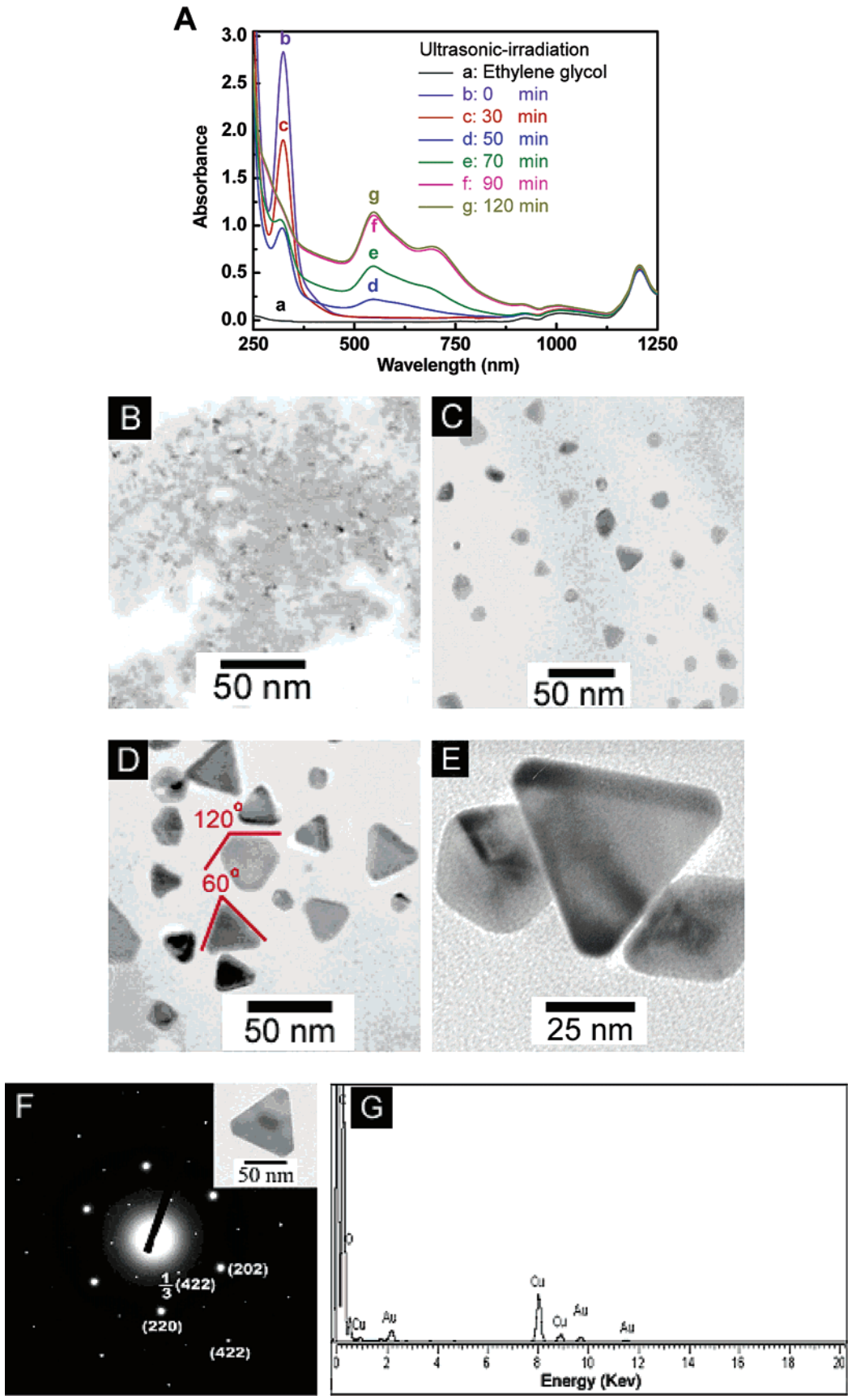

Figure 2. Optical absorption spectra (A) and the corresponding TEM images (B−F) for $HAuCl_4$ ethylene glycol solution ($HAuCl_4$, 0.5 mM; PVP, 200 mM) irradiated for a different time interval by ultrasonic wave: (B) and (C) after irradiation for 50 and 70 min, respectively, (D) and (E) irradiation for 120 min, (F) a single Au nanoprism and its corresponding SAED pattern, and (G) EDS results for a typical nanoprism on the copper grid (curve a in Figure 2A—for pure ethylene glycol).

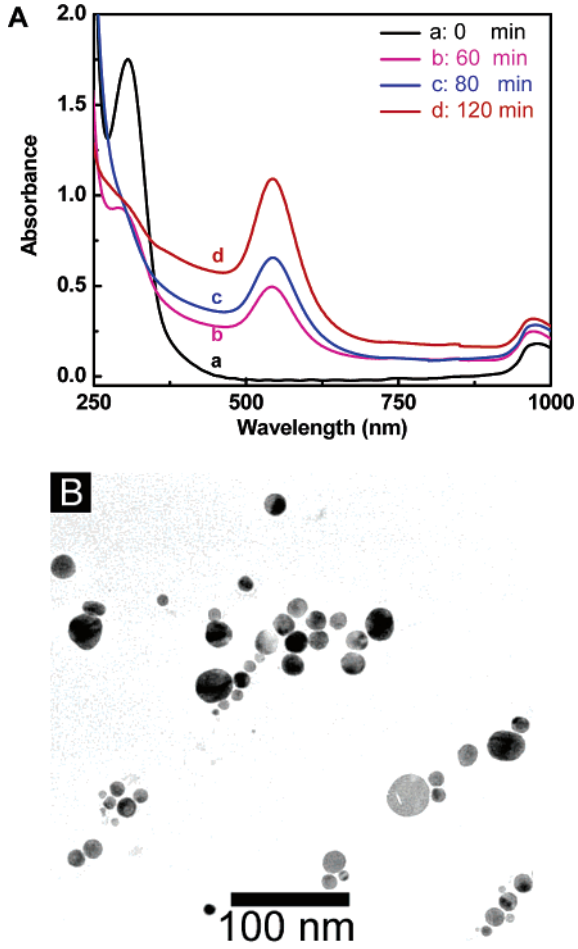

Figure 3. Optical absorption spectral evolution for $HAuCl_4$ aqueous solution ($HAuCl_4$, 0.5 mM; PVP, 200 mM) during ultrasonic irradiation (A) and the TEM image after irradiation for 120 min (B).

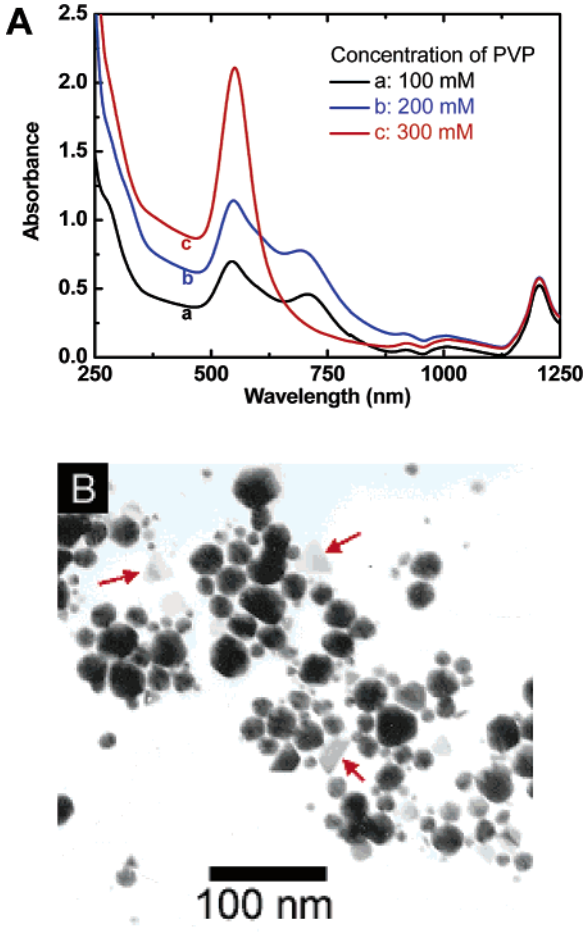

Figure 4. Optical absorption spectra (A) for the ultrasonic-irradiated samples with different PVP concentrations ($HAuCl_4$, 0.5 mM, irradiation for 120 min) and a TEM image for the sample with 300 mM PVP (B).

ions are gradually reduced in the aged-sample solution. Correspondingly, the in-plane absorption peak of Au nanoprisms gradually enhances and red shifts from 760 to 840 nm. The absorption peak at 545 nm enhances but does not shift. Similar time evolution results were also observed for the other aged samples after an addition of various amounts of $HAuCl_4$. Figure 7B presents the final optical spectra, more than one week after the addition of 0.1, 0.3, 0.5, and 1.0 mL of 25 mM $HAuCl_4$ to a 5 mL aliquot aged irradiated sample. The in-plane absorption of Au nanoprisms red shifts with an increase in the $HAuCl_4$ addition. TEM examination confirms that the size of Au nanoprisms increases with a rise in the $HAuCl_4$ addition, as shown in parts C−F of Figure 7. This means that we can manipulate the size of Au nanoprisms and hence the optical properties just by subsequent addition of a given amount of $HAuCl_4$ solution to the irradiated and aged Au nanoprisms colloidal solution.

4. Discussion

4.1. Formation of Au Nanoprisms. The chemical effect of ultrasonic irradiation originates from acoustic cavitation: formation, growth, and implosive collapse of bubbles, which leads to the decomposition of water or volatile precursors (RH) into hydrogen (H•) and hydroxyl (•OH) or reducing radicals (•R) owing to the production of high temperature and high pressure in collapsing cavities.[20] The radicals reduce $AuCl_4^-$ ions into Au° atoms which then start to nucleate and grow into nanoprisms, nanorods/nanowires, or nanoparticles, and so forth, when their concentration reaches the supersaturation value.[21,22]

As mentioned above, single-crystal Au nanoprisms were successfully synthesized in an ethylene glycol solution via a sonochemical approach. It is well-known that the formation of anisotropic nanostructures in the solution phase is normally related to the following two factors: One is surfactant-based soft templates, which can induce the preferential growth direction of the nanocrystal.[6,23] The other is selective adsorption of small molecules or polymers on certain crystal planes, which can control or confine the growth rate of the nanocrystals along a certain direction.[5,8−10,24−26] As we know, it is impossible for PVP to form a platelike soft template. Thus, we believe that the formation of platelike Au nanostructures is associated with the selective adsorption of the surfactant PVP and/or the reagent, solvent molecules on the preformed ultrafine Au nanocrystals.

The surfactant PVP is widely introduced as a stabilizer to prevent aggregation of the products in the synthesis of noble metal (Au, Ag, etc.) nanostructures. Furthermore, PVP can also influenced the growth rate of different crystallographic planes, by interacting with these planes through adsorption and desorption.[9,24−26] On the basis of this role of PVP, recently, many metallic nanostructures with well-controlled morphologies, such as Ag nanodisks,[9,10c] nanocubes,[24] nanowires,[24b,25] and platonic Au nanoparticles,[26] have been successfully synthesized. For gold, as demonstrated by Tsuji et al.[9] and Kim et al.[26] (here, it should be mentioned that their works were conducted in the ethylene glycol solution with no other reagents and surfactants

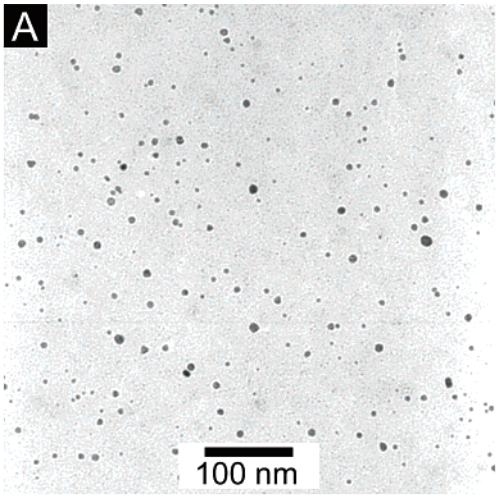

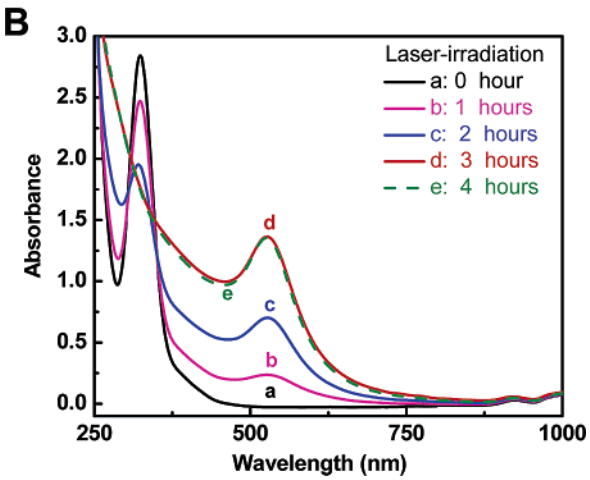

Figure 5. (A) TEM image of Au nanoparticles for 4 h laser-irradiated $HAuCl_4$ ethylene glycol solution ($HAuCl_4$, 0.5 mM; PVP, 200 mM). (B) Optical absorption spectra for laser-irradiated different time interval samples.

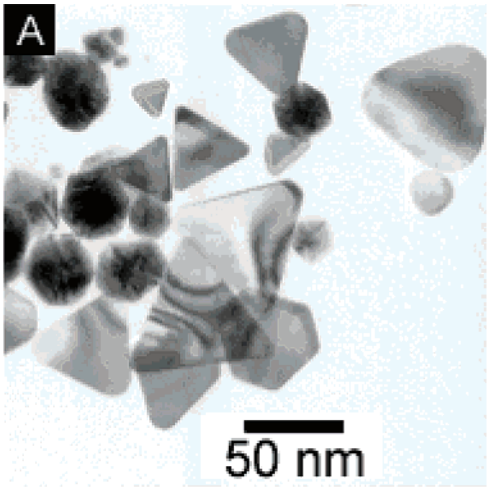

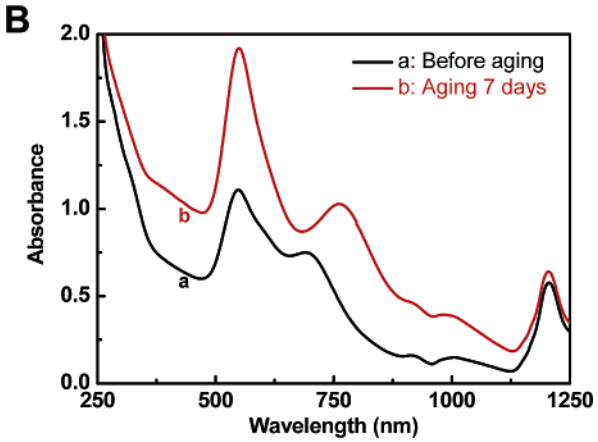

Figure 6. (A) TEM image of Au nanoprisms after aging for one week for the 120 min ultrasonically irradiated sample (Figure 2D). (B) The change of optical absorption spectra before and after aging.

except for $HAuCl_4$ and surfactant PVP), selective interaction between PVP and Au nanocrystals could greatly reduce the growth rate along the ⟨111⟩ direction and enhance the growth rate along the ⟨110⟩ direction, which can facilitate the formation of the platelike or other anisotropic Au nanostructures. In this study, the PVP concentration in the range from 100 to 200 mM is enough to induce dominant Au nanoprisms (see Figures 2 and 4A). At a higher PVP concentration (say, 300 mM), the high coverage of PVP limits the growth rate on all planes of gold nanocrystals, leading to an isotropic growth mode and, finally, spherical nanoparticle-dominant product (see Figure 4B). Conversely, PVP with an over-low concentration is also not favorable to the formation of Au nanoprisms owing to the less PVP adsorption. In the absence of PVP especially, Au nanoparticles are easily aggregated due to lacking protection of the surfactant. Obviously, the selective interaction between the surfactant PVP and Au nanocrystals is related to the PVP concentration.

However, Au nanoprisms cannot be synthesized in the ethanol/water solution or pure aqueous solution even with a proper concentration PVP. That is, surfactant PVP does not play a shape-directing role in the synthesis process but prevents aggregation of an Au nanoparticle. So, it is reasonable to conclude that ethylene glycol also plays important role for the formation of platelike Au nanostructures though its exact role is still not clear. Here, we suggest, although there is no direct experimental data available, that in addition to the selective interaction between the surfactant PVP and Au nanocrystals, ethylene glycol molecules, like surfactant PVP, can adsorb preferentially on the sites of the {111} planes of Au nuclei, which greatly decreases the surface energy of {111} planes and leads to preferential growth in the ⟨110⟩ direction. This, in turn, assists the formation of triangular and hexagonal platelike Au nano-objects.

As for ultrasonic irradiation, the acoustic cavitation occurs locally and instantaneously in solution (several micrometers in dimension and sub-microsecond in time scale, respectively).[27] So, the growth environment produced by ultrasonic-irradiation is relatively mild. In this case, Au nuclei can easily grow along preferred orientation and result in the formation of platelike particles due to the crystal-plane-dependent surface energy as well as the selective interaction between the surfactant PVP (and/or ethylene glycol molecules) and the different crystallographic planes of Au nanocrystals.[28] Whereas, the chemical effect of laser irradiation comes from rapid multiphoton absorption and local high-temperature plasma,[29] leading to the thermal decomposition and reduction of $AuCl_4^-$ ions. The reaction is prompt enough and thus results in the isotropic growth of Au nuclei, which induces the nearly spherical Au nanoparticles. In other words, ultrasonic irradiation provides a benign condition, leading to quasi-equilibrium crystal growth, while laser irradiation induces a severe growth condition, leading to equal-axis

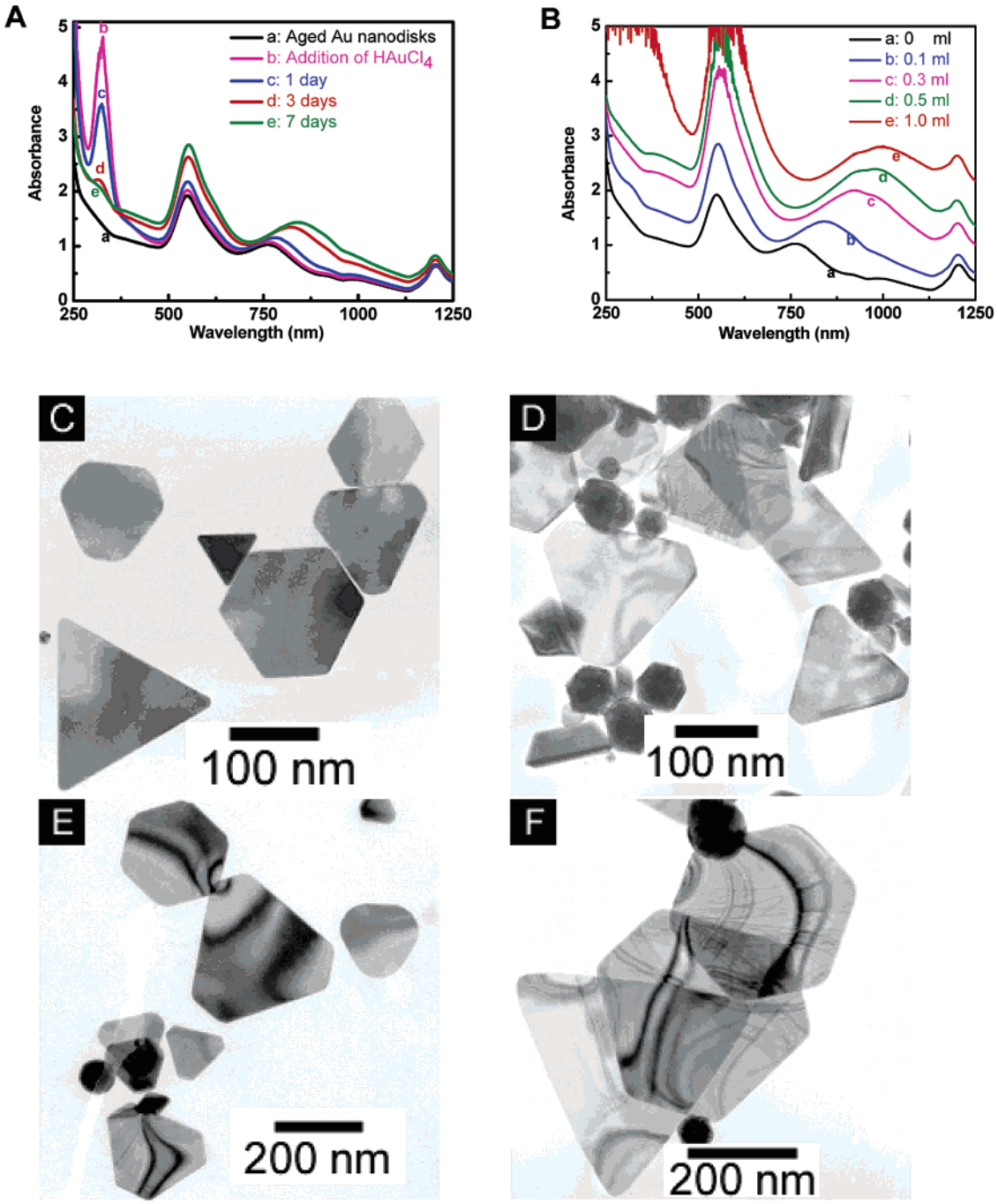

Figure 7. (A) Time evolution of optical absorption spectra for the aged irradiated sample (5 mL, ultrasonic-irradiated for 120 min, and then aged at room temperature for 7 days) after an addition of 0.1 mL of 25 mM $HAuCl_4$ solution. (B) The optical spectra for the samples with an addition of different amounts of $HAuCl_4$ after 7 days. (C−F) The TEM images of Au nanoprisms after 7 days for the samples, respectively, corresponding to the addition of 0.1, 0.3, 0.5, and 1 mL of 25 mM $HAuCl_4$ solution to a 5 mL aliquot aged sample.

growth. This implies that the formation of Au nanoprisms also profits from the benign condition provided by ultrasonic irradiation.

4.2. Further Growth of Au Nanoprisms. After ultrasonic irradiation for 120 min, there exist Au° atoms and Au clusters in the solution in addition to the Au nanoprisms formed during irradiation. During the subsequent aging, the formed Au nanoprisms will serve as "seeds" and grow, by attachment of the Au° atoms remaining in the solution or coming from Au clusters via a so-called oxidative Ostwald ripening process,[30,31] along the ⟨110⟩ direction due to high surface energy and weak adsorption of the surfactant PVP on the {110} planes,[9,25] leading to the increase of the planar dimension. After exhaustion of the remaining Au° atoms and Au clusters in the solution, further aging cannot increase the size of the Au nanoprisms.

$AuCl_4^-$ ions can be reduced by ethylene glycol, especially in the presence of Au nanoprisms and Au nanoparticles since the reduction potential of gold ions on the surface of nanostructured gold is positive compared to that of Au atom.[32] In addition, our previous work[33] revealed that the surfactant PVP was also a good reductant of gold ions in addition to a stabilizer. So, $AuCl_4^-$ ions can be reduced in the aged Au colloidal solution without any treatment (see Figure 7A), which provides the Au resource and induces the further growth of Au nanoprisms. Therefore, the size and hence the optical properties of Au nanoprisms can be manipulated via this strategy.

5. Conclusions

In summary, single-crystal gold nanoprisms with triangular or hexagonal shape, 30−40 nm planar dimension, and 6−10 nm thickness were successfully synthesized in an ethylene glycol solution via a simple sonochemical approach. The basal surfaces of the Au nanodisk are atomically flat {111} planes and the lateral surfaces are {110} planes. The formation of such nanoprisms is attributed to ethylene glycol molecules and PVP adsorbed preferentially on the {111} planes of Au nanocrystals as well as the benign condition provided by ultrasonic irradiation. The subsequent aging can induce the continuous growth of Au nanoprisms from 30 to 70 nm in size due to the existence of residual reduced Au° atoms and Au clusters in the solution. Further growth of Au nanoprisms from 70 to 400 nm in planar dimension is realized, and hence, the optical properties are manipulated, by adding a given amount of $HAuCl_4$ to the irradiated and aged Au nanoprisms colloid, which provides a simple and an effective method to synthesize Au nanoprisms with different sizes. Deficiency of this method is that the yield of product is not high since this approach is only suitable for the solution with a low $HAuCl_4$ concentration and benign environmental condition.

Acknowledgment. This study was supported by National Project for Basic Research (Grant No. 2006CB300402).

References and Notes

(1) Daniel, M. C.; Astruc, D. *Chem. Rev.* **2004**, *104*, 293−346.

(2) (a) Kim, J.; Cha, S.; Shin, K.; Jho, J. Y.; Lee, J. C. *Adv. Mater.* **2004**, *16*, 459−464. (b) Sun, X. P.; Dong, S. J.; Wang, E. K. *Langmuir* **2005**, *21*, 4710−4712. (c) Li, Z.; Liu, Z.; Zhang, J.; Han, B.; Du, J.; Gao, Y.; Jiang, T. *J. Phys. Chem. B* **2005**, *109*, 14445−14448. (d) Li, C. C.; Cai, W. P.; Cao, B. Q.; Sun, F. Q.; Li, Y.; Kan, C. X.; Zhang, L. D. *Adv. Funct. Mater.* **2006**, *16*, 83−90.

(3) (a) Shankar, S. S.; Rai, A.; Ankamwar, B.; Singh, A.; Ahmad, A.; Sastry, M. *Nat. Mater.* **2004**, *3*, 482−488. (b) Shankar, S. S.; Rai, A.; Ahmad, A.; Sastry, M. *Chem. Mater.* **2005**, *17*, 566−572.

(4) Millstone, J. E.; Park, S.; Shuford, K. L.; Qin, L. D.; Schatz, G. C.; Mirkin, C. A. *J. Am. Chem. Soc.* **2005**, *127*, 5312−5313.

(5) (a) Jin, R. C.; Cao, Y. W.; Mirkin, C. A.; Kelly, K. L.; Schatz, G. C.; Zheng, J. G. *Science* **2001**, *294*, 1901−1903. (b) Jin, R. C.; Cao, Y. W.; Hao, E.; Métraux, G. S.; Schatz, G. C.; Mirkin, C. A. *Nature* **2003**, *425*, 487−490. (c) Métraux, G. S.; Mirkin, C. A. *Adv. Mater.* **2005**, *17*, 412−415.

(6) (a) Maillard, M.; Giorgio, S.; Pileni, M.-P. *Adv. Mater.* **2002**, *14*, 1084−1086. (b) Chen, S. H.; Carroll, D. L. *Nano. Lett.* **2002**, *2*, 1003−1007. (c) Chen, S. H.; Fan, Z. Y.; Carroll, D. L. *J. Phys. Chem. B* **2002**, *106*, 10777−10781. (d) Maillard, M.; Giorgio, S.; Pileni, M.-P. *J. Phys. Chem. B* **2003**, *107*, 2466−2470. (e) Callegari, A.; Tonti, D.; Chergui, M. *Nano Lett.* **2003**, *3*, 1565−1568.

(7) (a) Sau, T. K.; Murphy, C. J. *J. Am. Chem. Soc.* **2004**, *126*, 8648−8649. (b) Mililigan, W. O.; Morriss, R. H. *J. Am. Chem. Soc.* **1964**, *86*, 3461.

(8) Malikova, N.; Pastoriza-Santos, I.; Schierhorn, M.; Kotov, N. A.; Liz-Marzán, L. M. *Langmuir* **2002**, *18*, 3694−3697. (b) Pastoriza-Santos, I.; Liz-Marzan, L. M. *Nano Lett.* **2002**, *2*, 903−905. (c) Liz-Marzán, L. M. *Mater. Today* **2004**, *7*, 26−31.

(9) (a) Tsuji, M.; Hashimoto, M.; Nishizawa, Y.; Tsuji, T. *Chem. Lett.* **2003**, *32*, 1114−1115. (b) Tsuji, M.; Hashimoto, M.; Nishizawa, Y.; Kubobawa, M.; Tsuji, T. *Chem.−Eur. J.* **2005**, *11*, 440−452.

(10) (a) Sun, Y. G.; Xia, Y. N. *Adv. Mater.* **2003**, *15*, 695−699. (b) Métraux, G. S.; Cao, Y. C.; Jin, R. C.; Mirkin, C. A. *Nano Lett.* **2003**, *3*, 519−522. (c) Jiang, L. P.; Xu, S.; Zhu, J. M.; Zhang, J. R.; Zhu, J. J.; Chen, H. Y. *Inorg. Chem.* **2004**, *43*, 5877−5883.

(11) (a) Pettinger, B.; Ren, B.; Picardi, G.; Schuster, R.; Ertl, G. *Phys. Rev. Lett.* 2004, **92**, 096101_1−096101_4. (b) Ren, B.; Picardi, G.; Pettinger, B.; Schuster, R.; Ertl, G. *Angew. Chem., Int. Ed.* **2005**, *44*, 139−142.

(12) (a) Maillard, M.; Huang, P.; Brus, L. *Nano Lett.* **2003**, *3*, 1611−1615. (b) Zhou, Y.; Wang, C. Y.; Zhu, Y. R.; Chen, Z. Y. *Chem. Mater.* **1999**, *11*, 1, 2310−2312. (c) Ibano, D.; Yokota, Y.; Tominaga, T. *Chem. Lett.* **2003**, *32*, 574−575.

(13) Sun, Y. G.; Mayers, B. T.; Xia, Y. N. *Nano Lett.* **2003**, *3*, 675−679.

(14) (a) Sun, X. P.; Dong, S. J.; Wang, E. K. *Angew. Chem., Int. Ed.* **2004**, *43*, 6360−6363. (b) Shao, Y.; Jin, Y. D.; Dong, S. J. *Chem. Commun.* **2004**, 1104−1105.

(15) (a) Naik, R. R.; Stringer, S. J.; Agarwal, G.; Jones, S. E.; Stone, M. O. *Nat. Mater.* **2002**, *1*, 169−172. (b) Liu, B.; Xie, J.; Lee, J. Y.; Ting, Y. P.; Chen, J. P. *J. Phys. Chem. B* **2005**, *109*, 15256−15263.

(16) Esumi, K.; Hara, J.; Aihara, A.; Usui, K.; Torigoe, K. *J. Colloid Interface Sci.* **1998**, *208*, 578−581.

(17) Kriebig, U.; Vollmer, M. *Optical Properties of Metal Clusters*; Springer-Verlag: Berlin, 1995.

(18) Kirkland, A. I.; Jefferson, D. A.; Duff, D. G.; Edwards, P. P.; Gameson, I.; Johnson, B. F. G.; Smith, D. J. *Proc. R. Soc. London, Ser. A* **1993**, *440*, 589−609.

(19) Germani, V.; Li, J.; Ingert, D.; Wang, Z. L.; Pileni, M. P. *J. Phys. Chem. B* **2003**, *107*, 8717−8720.

(20) (a) Makino, K.; Mossoba, M. M.; Riesz, P. *J. Am. Chem. Soc.* **1982**, *104*, 3537−3539. (b) Suslick, K. S. *Ultrasound: Its Chemical Physical and Biological Effects*; VCH: Weinheim, Germany, 1988.

(21) (a) Mullin, J. W. *Crystallization*, 3rd ed.; Oxford: 1997; chapter 5. (b) Nagata, Y.; Mizukoshi, Y.; Okitsu, K.; Maeda, Y. *Radiat. Res.* **1996**, *146*, 333−338.

(22) (a) Chen, W.; Cai, W. P.; Zhang, L.; Wang, G. Z.; Zhang, L. D. *J. Colloid Interface Sci.* **2001**, *238*, 291−295. (b) Kan, C. X.; Cai, W. P.; Li, C. C.; Zhang, L. D.; Hofmeister, H. *J. Phys. D: Appl. Phys.* **2003**, *36*, 1609−1614. (c) Fu, G. H.; Cai, W. P.; Kan, C. X.; Li, C. C.; Fang, Q. *J. Phys. D: Appl. Phys.* **2003**, *36*, 1382−1387. (d) Li, C. C.; Cai, W. P.; Kan, C. X.; Fu, G. H.; Zhang, L. D. *Mater. Lett.* **2004**, *58*, 196−199.

(23) Pileni, M.-P. *Nat. Mater.* **2003**, *2*, 145−150.

(24) (a) Sun, Y. G.; Xia, Y. N. *Science* **2002**, *298*, 2176−2179. (b) Sun, Y. G.; Xia, Y. N. *J. Am. Chem. Soc.* **2004**, *126*, 3892−3901. (c) Wiley, B.; Sun, Y. G.; Mayers, B.; Xia, Y. N. *Chem.−Eur. J.* **2005**, *11*, 454−436.

(25) (a) Sun, Y. G.; Gates, B.; Mayers, B.; Xia, Y. N. *Nano Lett.* **2002**, *2*, 165. (b) Sun, Y. G.; Yin, Y. D.; Mayers, B. T.; Herricks, T.; Xia, Y. N. *Chem. Mater.* **2002**, *14*, 4736.

(26) Kim, F.; Connor, S.; Song, H.; Kuykendall, T.; Yang, P. D. *Angew. Chem., Int. Ed.* **2004**, *43*, 3673−3677.

(27) Okitsu, K.; Yue, A.; Tanabe, S.; Matsumoto, H.; Yobiko, Y. *Langmuir* **2001**, *17*, 7717−7720.

(28) Buckley, H. E. *Crystal Growth*; Wiley: New York, 1951.

(29) (a) Zhao, C. J.; Qu, S. L.; Qiu, J. R.; Zhu, C. S.; Hirao, K. *Chem. Lett.* **2003**, *32*, 602−603. (b) Zhao, C. J.; Qu, S. L.; Qiu, J. R.; Zhu, C. S. *J. Mater. Res.* **2003**, *18*, 1710−1714.

(30) Mosseri, S.; Henglein, A.; Janata, E. *J. Phys. Chem.* **1989**, *93*, 6791−6795.

(31) Duff, D. G.; Baiker, A. *Langmuir* **1993**, *9*, 2301−2309.

(32) Jana, N. R.; Gearheart, L.; Murphy, C. J. *Chem. Mater.* **2001**, *13*, 2313−2322.

(33) Kan, C. X.; Cai, W. P.; Li, C. C.; Zhang, L. D. *J. Mater. Res.* **2005**, *20*, 320−324.